PEDESTRIAN RESPONSE WITH DIFFERENT INITIAL POSITIONS DURING IMPACT WITH A MID-SIZED SEDAN

Huipeng Chen
David Poulard
Jeff R. Crandall
Matthew B. Panzer
Center for Applied Biomechanics, University of Virginia
United States of America

Paper Number 15-0391

ABSTRACT

Real-world pedestrian impacts occur with highly-variable or unknown initial conditions of the pedestrian. However, experimental pedestrian tests and computational pedestrian impact simulations mainly focus on the response of the subject using specific initial conditions. The objective of this study is to investigate computationally the influence of posture and impact direction angle on pedestrian response during an impact. The 50th male THUMS pedestrian model was integrated with a mid-sized sedan finite element model initially travelling at 40 km/h. The influence of the pedestrian position during impact was investigated by varying 9 orientations (relative to the vehicle) and 3 standing/gait postures, for a total of 27 impact configurations simulated. Pedestrian kinematics and injury were assessed and compared across all simulations. Substantial variations were observed on the pedestrian torso rotation (-68.9°~57.6°), and head impact conditions (head impact time 111~139 ms, and head impact velocity 10.7~15.3 m/s). The head impact velocity was found to correlate with the impact direction angle, where facing towards or away from the vehicle would result in greater head impact velocity than when struck in a purely-lateral impact.

INTRODUCTION

Although significant improvements have been achieved in mitigating pedestrian fatalities, there are still over 400,000 pedestrians killed each year worldwide [1]. Epidemiological reviews have highlighted that 66-82% of pedestrians were hit by passenger cars and 60-77% of pedestrians were struck by the vehicle front [2], and serious injuries occur frequently at speeds between 25 and 55 km/h [3]. More than 60 % of the pedestrian accidents occurred at a vehicle speed of 40 km/h or less, and impacts with the bumper, hood, and windshield were believed to be the leading sources of pedestrian injury [4]. This suggests that an indepth understanding of the complex interaction between the pedestrian and vehicle is essential to ensure effective countermeasures.

The response of the human body to vehicle impact has been extensively studied using post-mortem human specimens (PMHS) on component tests [5] and vehicle-impact tests [6- 9]. These tests are the primary source of data for the development of physical and computational surrogates (anthropomorphic test devices and human body models, respectively). Understandably, studies involving vehicle-pedestrian impact using PMHS have focused on well-defined situations such as pure-lateral vehicle impact direction and specific pedestrian posture.

The most common pedestrian-vehicle impacts occur when pedestrians are crossing the road, and the amount of pedestrians struck laterally varies between 65-89% of all impact cases [2,3,10]. However, an accurate pedestrian impact angle may not always be reported and it is reasonable to assume that the pedestrian impact direction is not purely lateral. In addition, prior to an accident, pedestrians often move in different ways: 71-79 % of pedestrians involved in accidents are standing upright and moving across the road [11], while 65% of pedestrians are walking and 20% are running [2]. Reaction to an oncoming vehicle will also influence the initial orientation and posture of a pedestrian [12]. Changes to pedestrian orientation and posture from the purely-lateral stance may greatly affect the ensuing kinematics, injury risk, and pattern during a vehicle-pedestrian impact.

Compared to experimental tests performed with PMHS which differ in age and anthropometry, simulations with human computational models have the potential to evaluate the impact response of a single individual while introducing extrinsic variability. Peng et al. [13] used the stances for different gait parameters developed in a previous pedestrian sensitivity study by Untaroiu et al. [14] to investigate the effects of gait on pedestrian head

kinematics. However, this study did not investigate the whole-body kinematics and injury mechanism because a simplified multibody ellipsoid model was used. Finite element (FE) models of a human body offer some promising advantages for studying injury biomechanics, including the prediction of injury mechanisms and injury criteria and a large potential for customization. One the existing human body models (HBMs) that have been developed is the Total Human Model for Safety (THUMS) pedestrian model, which has been used to investigate the biomechanics of vehicle-pedestrian impact [15- 21]. While these studies focused on the risk of injury to a specific body part (brain: [19], shoulder: [21]) or the influence of specific parameters such as car type, vehicle speed, and pedestrian size [17-20], there were no studies on the influence of posture and impact orientation.

The hypothesis of this study is that changes to the pedestrian posture and orientation at the time of impact will significantly affect the resulting responses and distribution of injury predicted for the pedestrian. Thus, the objective of this study is to computationally investigate the influence of posture and impact orientation on pedestrian kinematics and injury during an impact with a mid-sized sedan.

METHODS

Model Setup

The THUMS pedestrian model (50th male, version 4.01) was integrated with a FE model of the front-end structure of a mid-sized sedan (Figure 1). The vehicle model is the same vehicle used in a previous experimental PMHS pedestrian test series at UVA reported by Subit et al. [9] . All boundary conditions and mass distributions assigned to the FE vehicle model were consistent with those of the test series. An initial velocity of 40 km/h was applied on the vehicle and was allowed to impact the pedestrian. The friction coefficient between the HBM and the vehicle was 0.5, and was 0.6 between the feet and ground [13]. The simulation time was 200 ms, using the code LS-DYNA v971 7.1.1.

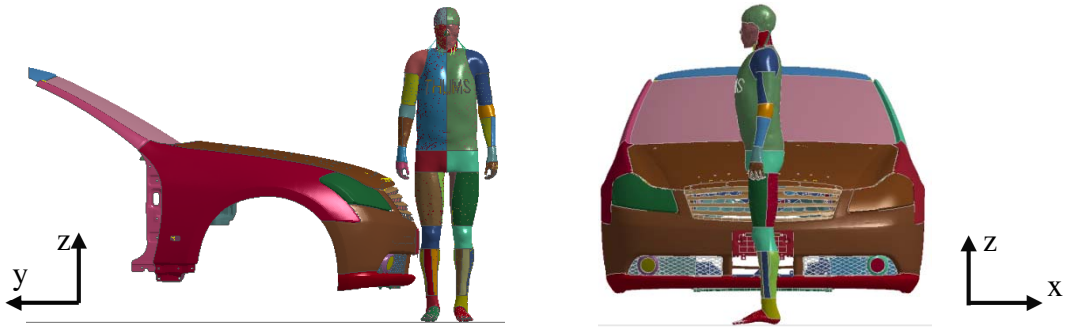

Figure1. Simulation set up (Baseline model S0).

Alteration of posture

Three human postures were created from the original HBM (Figure 2). A baseline model “S”, which is the default position of the THUMS pedestrian model, was defined as a standing posture with arms down and legs aligned. Two additional models were defined with walking postures, referred to as “RF” and “LF”, and were derived from a normal gait-cycle of 0% (right leg forward) and 50% (left leg forward) respectively [14]. Positioning of the THUMS pedestrian model for the RF and LF postures was done using pre-simulation to match the angles of the hips, knees, shoulders and elbows.

Standing (S) *Right leg forward (RF)* *Left leg forward (LF)*

Figure 2. Pedestrian postures.

Impact direction

Nine pedestrian impact orientations were defined in the study, with the pedestrian center of gravity (CG) located along the centerline of the vehicle. The baseline impact orientation was the pure-lateral case (Figure 1) with an associated impact direction angle of 0 degrees. Eight additional impact directions were created from the baseline orientation by rotating the pedestrian relative to the vehicle by ±15° ("near lateral"), ±30° and ±60° ("non-lateral"), and ±90° ("facing toward" or "facing away") (Figure 3). Due to the nearly symmetric geometry of the vehicle and HBM, these cases represent a full 360° array of pedestrian impact orientation relative to the vehicle.

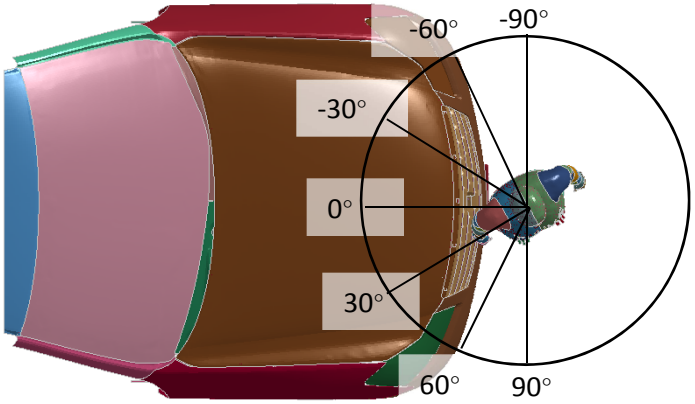

Figure3. Impact direction angles. The model shown is S30.

Simulation matrix

By varying the three pedestrian postures and nine impact directions, a matrix of 27 cases in total was created and simulated (Table 1).

Table 1. Simulation Matrix

	Simulation ID								
Impact direction angle	**0**	**15**	**30**	**60**	**90**	**-15**	**-30**	**-60**	**-90**
Standing posture	S0	S15	S30	S60	S90	SN15	SN30	SN60	SN90
Right leg forward posture	RF0	RF 15	RF 30	RF 60	RF90	RFN15	RFN30	RFN60	RFN90
Left leg forward posture	LF0	LF15	LF30	LF60	LF90	LFN15	LFN30	LFN60	LFN90

Pedestrian Kinematics

Head impact velocity V_h was defined as the relative velocity between the head center gravity and the vehicle CG after initiation of contact (Equation 1). The head impact location was categorized by 4 areas on the vehicle according to the wrap around distance (WAD) [23], which was measured as the sum of the distance from the ground to bumper, bumper to hood leading edge, and hood leading edge to head impact location. For the vehicle used in this study, the head impact location could be classified by the 4 areas illustrated on Figure 4.

$$V_{relative} = |\vec{V}_{head} - \vec{V}_{car}| \qquad \text{[Equation 1]}$$

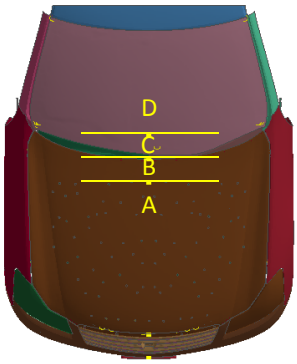

Figure4. Wrap around distance (WAD) categories. A: WAD < 1800 mm (hood), B: 1800 ⩽ WAD<1950 (cowl), C: 1950 ⩽ WAD< 2100 (windshield frame), D: WAD ⩾ 2100 mm (windshield).

Torso rotation was calculated by change in the line formed by the left and right acromion, from the initial and final (when torso impacts vehicle) pedestrian facing angle to the vehicle (Equation 2) and Figure 5.

$$\theta_{initial} = accsin(\frac{L_x}{L}) \qquad \theta_{final} = accos(\frac{L_z}{L}) \qquad \text{[Equation 2]}$$

Figure5. Initial torso angle and final torso angle (Configuration SN30).

Bony Fracture and Ligament rupture

The injuries predicted to occur in the simulations were bone fractures and ligament ruptures, and strain-based injury criteria were used for predicting these types of injuries. A 3% principal strain fracture criterion was used to predict all the cortical bone fracture (except for hands and feet), and 16% principal strain injury criterion was used for knee ligament rupture [20, 22]. These values are representative of a 40 year-old subject [20]. Tissue-level injury prediction was done in the post-processing stage of the simulation, since element deletion was not activated during the simulations to ensure stability of the models.

Statistical Analyses

The response variables in this study were the pedestrian kinematics obtained from the models: head impact time, head impact site, head velocity Vh, torso impact angle, torso rotation. Descriptive statistics were given for all variables as mean ± one standard deviation (SD). Posture and impact direction effects were explored using a general linear regression model with the pedestrian kinematics as the dependent variables. Student's t-tests were performed on the regressed coefficients and $p < 0.05$ was considered statistically significant.

RESULTS

Pedestrian Kinematics

Pedestrian kinematics for each simulation are listed in Table 2. Considerable variability was found with the observed head impact time of 111~139 ms, head impact velocity of 10.7~15.3 m/s, and torso rotation of -68.9°~57.6°. All head impact locations were between the cowl and windshield frame, with the WAD ranging from 1900 to 2100 mm. In all 27 configurations, 8 experienced shoulder impact, and 14 experienced elbow impact (4 experienced both), while only 9 did not experience either impact. In Figure 6, V_h is displayed crossed impact direction angle and absolute impact direction angle according to the respective posture. The head impact velocity V_h was higher in cases where the pedestrian was turned away from the purely-lateral orientation (Figure 6). No trend was observed for the amount of torso rotation experienced by the pedestrian as a factor of impact direction angle (Figure 7).

Linear regression coefficients of the pedestrian kinematics are shown in Table 3. Posture was a significant predictor for head impact site ($p=0.029$), torso impact angle ($p=0.049$) and torso rotation ($p=0.049$). Impact direction angle was a significant predictor for head impact site ($p<0.0001$) and torso impact angle ($p<0.0001$). There was a trend that impact direction may be predictor for head impact velocity V_h ($p=0.066$). The absolute impact direction angle was found to be a significant predictor ($p<0.0001$) for the head impact velocity Vh.

Table 2. Pedestrian kinematics

Cases	Head impact time (ms)	Head impact site	Head impact location	V_h (m/s)	Torso impact angle (°)	Torso rotation (°)	Upper extremity impact
S0	139	lateral	C	11.6	15	15	both
S15	139	occipital	C,D	10.8	72.6	57.6	elbow
SN15	135	frontal	C	10.8	-83.9	-68.9	elbow
S30	134	occipital	C	11.8	84.0	54.0	elbow
SN30	125	frontal	C	12	-89.0	-59.0	elbow
S60	123	occipital	C	14.6	77.6	17.6	-
SN60	117	frontal	B,C	13.4	-88.3	-28.3	-
S90	117	occipital	C	15.3	87.9	-2.1	-
SN90	111	frontal	B	14.0	-88.6	1.4	-
RF0	128	occipital	C	12.2	29.5	29.5	shoulder
RF15	124	occipital	C	12.7	47.6	32.6	shoulder
RFN15	129	lateral	B,C	13.6	8.5	23.5	shoulder
RF30	125	occipital	B,C	12.7	75.5	45.5	elbow
RFN30	129	lateral	B	14.9	-27.0	3.0	shoulder
RF60	123	occipital	B,C	13.5	77.5	17.5	elbow
RFN60	130	frontal	B,C	12.5	-86.5	-26.5	-
RF90	130	occipital	B	15	87.0	-3.0	-
RFN90	129	frontal	B,C	13.3	-75.0	15.0	-
LF0	132	frontal	C	11.7	-40.0	-40.0	both
LF15	132	lateral	C	12.5	11.8	-3.2	both
LFN15	131	frontal	C	11.2	-76.0	-61.0	elbow
LF30	130	lateral	B,C	13.9	23.9	-6.1	both
LFN30	118	frontal	B,C	10.7	-77.6	-47.6	elbow
LF60	134	occipital	B,C	13.3	90.0	30.0	-
LFN60	124	frontal	B	12.1	-52.2	7.8	elbow
LF90	132	occipital	B, C	15.4	88.2	-0.8	-
LFN90	129	frontal	B	13.2	-106.0	-16.0	elbow

*A: WAD < 1800 mm (hood), B: 1800 ⩽ WAD<1950 (cowl), C: 1950 ⩽ WAD< 2100 (windshield frame), D: WAD ⩾ 2100 mm (windshield).

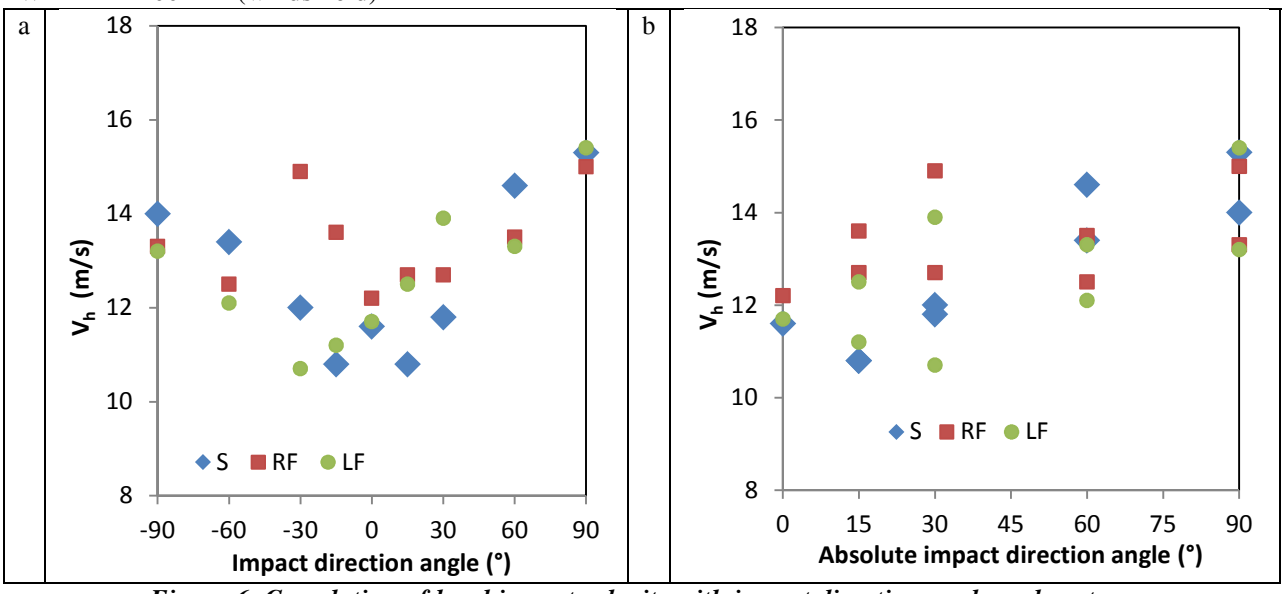

Figure 6. Correlation of head impact velocity with impact direction angle and posture

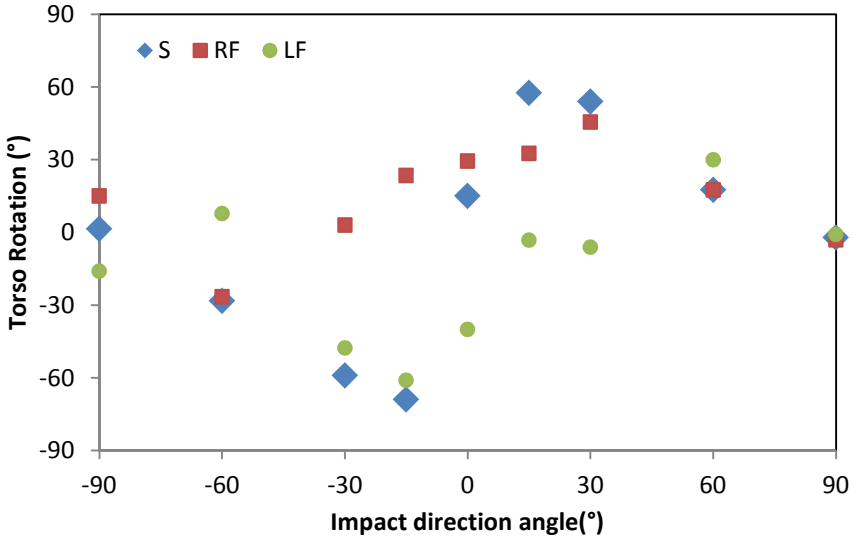

Figure7. Correlation of torso rotation with impact direction angle and posture

Table 3. Linear regression analysis of pedestrian kinematics

Variables	Coefficients	S.D.	t-Stat	P-value	Lower 95%	Upper 95.0%
Head impact time						
Posture	-0.83	1.60	-0.52	0.607	-4.13	2.46
Impact direction angle	0.03	0.02	1.04	0.310	-0.03	0.08
Head impact site						
Posture*	-0.33	0.14	-2.32	0.029	-0.63	-0.04
Impact direction angle*	-0.01	0.00	-6.39	0.0000	-0.02	-0.01
Head impact velocity V_h						
Posture	0.36	0.31	1.15	0.263	-0.28	1.00
Impact direction angle	0.01	0.00	1.92	0.066	0.00	0.02
Absolute impact direction angle*	0.03	0.01	4.94	0.000	0.02	0.04
Torso impact angle						
Posture*	15.28	7.36	2.08	0.049	0.09	30.46
Impact direction angle*	1.19	0.11	10.61	0.0001	0.96	1.43
Torso rotation angle						
Posture*	15.22	7.36	2.07	0.049	0.04	30.40
Impact direction angle	0.19	0.11	1.73	0.097	-0.04	0.43

*p< 0.05

Bony Fracture and Ligament Rupture

The observed cortical bone fractures and knee ligament ruptures are listed in Table 4. The skeletal fractures and ligament ruptures were mainly found in the skull and knee ligaments. Skull fractures were observed in every case except three cases (cases S15, R30, and RN30). Only two upper neck (C2) fractures were observed, and one of them (case RFN30) experienced a shoulder impact causing the neck to sustain a substantial bending moment. In three cases, there was a single rib (upper thorax) fracture and in one case a sternum fracture was observed. Only one upper extremity fracture (right ulna during an elbow impact in S30) and two thoracic spine fractures occurred. Shoulder injuries were found and included four cases of scapular fracture and one clavicle fracture. All cases with shoulder injury experienced oblique torso impact with the hood (facing down, with torso impact angle -40°~ -76°), but in the case RFN90 and LFN60, the scapula fractures did not happen on the impacted side.

Pelvis fractures occurred in four cases, all on the right acetabulum occur. Those cases were pure-lateral or near-lateral impacts. There were no thigh and leg fracture observed in these cases, and in all cases except S90 a knee ligament rupture occurred. There was a correlation between the number of knee ligament ruptures and the impact direction (Figure 8). Most knee ligament ruptures occurred when the pedestrian was facing towards the vehicle (creating a hyperextension of the knees) and least ruptures occurred when the pedestrian was facing away from the vehicle (creating a flexion of the knees).

Table 4. Bony fractures and ligament ruptures

Cases	Head/ Neck	Upper Extremity	Chest/spine /shoulder	Pelvis	Thigh /Leg	Knee ligaments rupture (R/L/Number)
S0	Skull/-	-	-	R Hipbone Acetabulum	-	(ACL, MCL)/ (ACL, PCL, LCL)/5
S15	-	-	Sternum, L 1st rib /-/-	-	-	(ACL, MCL)/(ACL, LCL)/4
SN15	Skull/-	-	-	-	-	(All)/(ACL, LCL, PCL)/7
S30	Skull/-	R ULNA	-	-	-	(MCL)/(LCL, ACL)/3
SN30	Skull/-	-	-	-	-	(MCL,ACL,PCL)/(ACL,LCL,PCL),6
S60	Skull/-	-	-	-	-	/(ACL, LCL)/2
SN60	Skull/-	-	-	-	-	(All)/(ACL, LCL, PCL)/7
S90	Skull/-	-	-	-	-	-/-/0
SN90	Skull/-	-	-	-	-	All/All/8
RF0	Skull/-	-	-	R Hipbone Acetabulum	-	(ACL, MCL)/ (ACL, LCL)/4
RF15	Skull/-	-	-	-	-	(MCL)/(ACL, LCL)/3
RFN15	Skull/-	-	-	-	-	(MCL,ACL,PCL)/(ACL,LCL)/5
RF30	-	-	R 2nd rib/-/-	-	-	(MCL)/(LCL, ACL)/3
RFN30	-/C2	-	-	-	-	(MCL, ACL, PCL)/ (ACL, PCL, LCL)/6
RF60	Skull/-	-	-	-	-	-/(ACL, LCL)/2
RFN60	Skull/-	-	-	-	-	(MCL, ACL, PCL)/(All)/7
RF90	Skull/-	-	-	-	-	(LCL)/-/1
RFN90	Skull/-	-	-/-/L scapula	-	-	All/All/8
LF0	Skull/-	-	-/-/R scapula	R Hipbone Acetabulum	-	(ACL, MCL)/ (ACL, LCL, PCL)/5
LF15	Skull/-	-	R 3rd rib/T3/-	-	-	(MCL)/(ACL, LCL, PCL)/4
LFN15	Skull/-	-	-/-/R clavicle, R scapula	R Hipbone Acetabulum	-	(ACL, MCL)/ (ACL, LCL, PCL)/5
LF30	Skull/-	-	-/T3/-	-	-	(ACL,MCL)/(ACL,LCL,PCL)/5
LFN30	Skull/-	-	-	-	-	(ACL,MCL,PCL)/(ACL,LCL,PCL)/6
LF60	Skull/-	-	-	-	-	(ACL, LCL)/(ACL, LCL)/4
LFN60	Skull/-	-	-/-/R scapula	-	-	(ACL,MCL,PCL)/(ACL,LCL,PCL)/6
LF90	Skull/C2	-	-	-	-	-/(LCL)/1
LFN90	Skull/-	-	-	-	-	(ACL, LCL, PCL)/(All)/7

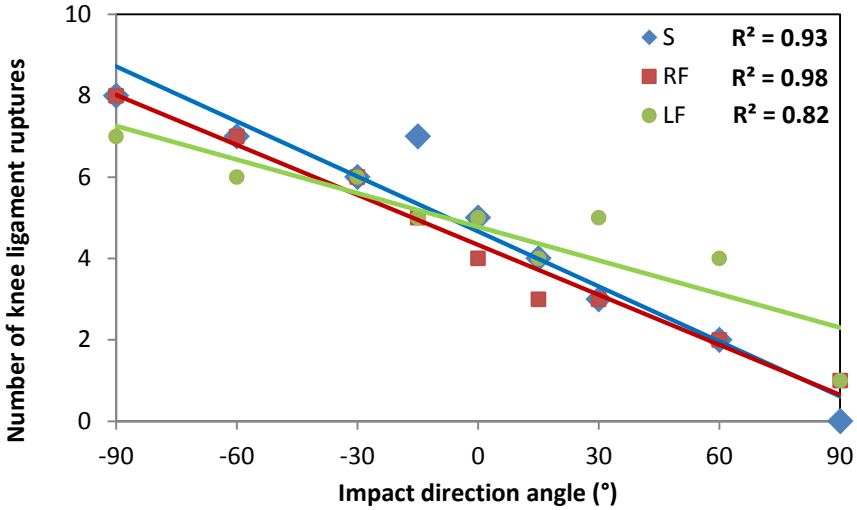

Figure 8. Correlation of the number of knee ligament ruptures with impact direction angle and posture.

DISCUSSION

Pedestrian Kinematics

Torso rotation Pedestrian torso rotation was caused by the impact of the vehicle initially striking the pedestrian leg at a location away from the body CG, which depended on the initial impact direction and human posture. Generally, a positive initial impact orientation caused positive torso rotation and vice versa. For the standing posture cases, the torso rotation entirely depended on the initial impact direction. However, for the right leg forward (RF) and left leg forward (LF) cases, the torso rotations were jointly determined by the initial impact direction and human posture. In RF cases, the initial contact point was anterior to the body CG even in pure-lateral impact, and as a result, case RF0 obtained 29.5° torso rotation; while in LF cases, the initial contact point was posterior to the body CG in pure-lateral impact, and case LF0 obtained -40° torso rotation. Consequently, only one negative torso rotation was observed in all 9 RF cases, and only two positive torso rotations were observed in all LF cases (Figure 7).

Shoulder impact and elbow impact In most of the pedestrian experimental tests [6-9], the PMHS hands were attached to each other prior to the pure-lateral impact. As a result, substantial elbow impact and shoulder impact were seen in the tests conducted [6-8]. In this study, the occurance of shoulder impact depended on the initial impact direction. All the cadaver tests were pure-lateral impact and all experienced shoulder impact. In the simulations, fewer shoulder impacts were observed and they were mainly from cases with a purely-lateral or near-lateral orientation. The occurance of elbow impact depended on both the initial impact direction and arm posture. Eleven of 14 cases with elbow impacts occurred with an initial impact direction from 0° ~ 30°. The cases with right leg forward (RF) posture (Figure 1-2) had less occurrence of elbow impact. All those cases without shoulder or elbow impact were with initial impact angles of ±60° and ±90°.

The experiments revealed that elbow and shoulder impacts had considerable influence on head kinematics [6-9]. Elbow impact influences torso rotation and changes the proceeding head kinematics. In the simulations, those configurations with elbow or shoulder impact had much lower head impact velocity (12.3±1.2 m/s, while 14.1±1.0 m/s for cases without elbow or shoulder impact) and later head impact time (average 129.2±5.5 ms, while average 124.8±8.1 ms for cases without elbow or shoulder impact).

Head impact condition In 11 cases, the head impact sites are at the occipital portion of the head, and in the other 11 cases the head impacts are frontal portion of the head. Only 5 of 27 cases resulted in a lateral impact to the head. Different phenomenon can explain this finding. Firstly, facing toward or away from the vehicle resulted in the head impact direction in the frontal and occipital regions respectively. Secondly, the torso rotation, due to the initial impact direction and human posture, resulted in the oblique torso impact with the hood. The torso would continue to rotate around the shoulder during the impact which resulted in the head impact striking the vehicle either in the frontal portion of the head or the occipital portion, not an oblique

impact (posterior-lateral or anterio-lateral). In a typical example (case RF15), the pre-impact, shoulder-impact, and head impact shown in Figure 9, and illustrates the torso rotation and the following head impact. Consequently, the lateral head impacts only happen when the torso impact was lateral (S0, RFN15, RFN30, LF15 and LF30), which account for a very low proportion of the simulated cases (5/27). Interestingly, the head impact velocity of cases resulting in occipital head impacts was 13.4±1.5 m/s, while cases with frontal head impact was slightly lower at 12.3±1.1 m/s.

0 ms (torso yaw 15°) *110 ms (torso yaw 47.6°)* *135 ms (torso yaw 63.1°)*

Figure 9. Torso rotation and head impact direction (case RF15).

The head impact velocity was sensitive to the initial impact direction, and increased as the initial impact angle increased (in magnitude). The head impact velocity was 11.8±0.3 m/s in pure-lateral impact, 11.9±1.2 m/s in near-lateral impact, 13.0±1.2 m/s in non-lateral impact, and 14.4±1.0 m/s in facing toward and facing away impacts. The head impact velocity was not sensitive to human posture, and was 12.7±1.67 m/s in standing postures, 13.4±1.0 m/s in RF postures, and 12.7±1.5 m/s in LF postures.

Directional dependence In standing and LF posture cases, the near-lateral cases had different torso rotation than pure-lateral cases. The head velocity was found to correlate with the impact direction angle ($p=0.029$). Since the head impact velocity was found to greatly influence the head injury risk [22], the head injury risk might be substantially influenced by the impact direction angle.

Posture dependence The directions of torso rotation were fundamentally different for various postures; torso rotation was found correlated to the posture ($p=0.049$). Therefore evaluating a pedestrian model in only one posture as in previous studies [18, 20] may not sufficiently encompass all likely head injury responses.

Bony Fracture and Ligament Rupture

Frequent skull fractures in these simulation could be attributed to the high stiffness of the impact locations (cowl and windshield frame) and the severity of the vehicle impact. In one of the three cases without skull fracture (S15), the head contacted the windshield, which is the softest area in all the head impact locations in this study. In the studies by Watanabe et al. [19, 20], skull fracture was not observed in centerline impact (at 40 km/h), but observed in corner impacts in which the head impact location was the A pillar. In the simulation study by Han et al., more than 70% AIS 4+ head injury risk (based on HIC value) was observed for a 50th percentile male impacted by a medium-sized sedan (centerline) at 40 km/h.

Very few rib fractures were observed in this study, but this is consistent with the pedestrian impact literature. In a simulation study by Han et al., the risk of chest injury was low [17, 18]. Likewise, no rib fractures were observed in the studies by Watanabe et al. [19, 20]. In the PMHS experiments, Subit et al. reported that subjects impacted by the small city car sustained more rib fractures than the subjects impacted by the mid-sized sedan [9].

In this study, the height of pedestrian knee was approximately at the center of the vehicle bumper causing a substantial bending effect at the knee joint and exposing the knee to severe impact. Knee ligament injury was very sensitive to impact direction. The most severe knee injuries were in the facing toward impacts where the knee was hyperextended, while the facing away impact rarely resulted in knee ligament ruptures because the knee flexed. In most of pure-lateral and near-lateral impacts, the valgus knee sustained MCL an ACL rupture,

and the varus knee sustained ACL and LCL rupture. As a result, ACL was the most frequently injured knee ligament in the pedestrian impacts because it happens on both knees, while MCL ruptures were mainly on valgus knee and LCL were mainly on varus knee.

Limitations

In this study, the influence of pre-crash posture was investigated using a standing posture and two walking postures representing the most distinct upper and lower extremity postures during the entire gait cycle [14]. An extension of this study, where intermediate gaits are added to the study will help to confirm the results presented in this paper.

The vehicle model was designed to reproduce the pedestrian impact buck used in Subit et al. [9] and did not contain an engine which might affect the pedestrian kinetics while in contact with the hood. However in another pedestrian impact study, Han et al. reported that the clearance between the hood and the engine in a mid-sized sedan was large enough to prevent the hood from impacting against the engine during a pedestrian impact [17, 18].

Finally, injury modeling using element deletion was not used to ensure numerical stability of the model. Thus, the results of this study would rely on the assumption that the influence of bone fracture on the ensuing pedestrian kinematics and kinetics would be negligible.

CONCLUSIONS

In the present study, a 50^{th} pedestrian human body model was subjected to impact with the centerline of a mid-sized sedan at 40 km/h. Three postured models were created from the original HBM: one matching the standard posture and two matching extreme walking gait postures. Nine impact directions were also investigated. A substantial variety of responses was observed when the impact direction and human posture were varied, including the pedestrian torso rotation, head impact condition, and knee ligament rupture. The patterns observed in the responses of the postured HBM indicate that the shoulder and elbow impact occurred frequently and substantially influenced the head kinematics. The head impact velocity was found to correlate with the impact direction angle, where facing towards or away from the vehicle would result in greater head impact velocity than when struck in a purely-lateral impact.

ACKNOWLEDGEMENTS

The authors would like to acknowledge support from Toyota Collaborative Safety Research Center (Toyota CSRC). The authors would like to acknowledge Aaron Steinhilb and Robert Panek (Toyota Motor Engineering & Manufacturing, North America) for their contribution to the design of the study. Note: the views expressed in this paper are those of the authors and do not necessarily represent or reflect the views of the sponsors.

REFERENCES

[1] Naci, H., Chisholm, D., and Baker, T. D. 2009. “Distribution of road traffic deaths by road user group: a global comparison”. Injury Prevention, 15(1), 55-59.
[2] Hardy, R. 2009. "APROSYS - Final Report for the Work on "Pedestrian and Pedal Cyclist Accidents" (SP3), AP-90-0003", Cranfield Impact Centre.
[3] Yang, J. 2005. “Review of injury biomechanics in car-pedestrian collisions”. International Journal of Vehicle Safety, 1(1), 100-117.
[4] Chen, H.P., Fu, L.X., and Zheng, H.Y. 2009. “A comparative study between China and IHRA for the vehicle-pedestrian impact”, SAE International Journal of Passenger Cars-Mechanical Systems 2, 1108–1115.
[5] Kerrigan, J. R., Drinkwater, D. C., Kam, C. Y., Murphy, D. B., Ivarsson, B. J., Crandall, J. R., and Patrie, J. 2004. “Tolerance of the human leg and thigh in dynamic latero-medial bending”. International Journal of Crashworthiness, 9(6), 607-623.
[6] Schroeder, G., Konosu, A., Ishikawa, H., and Kajzer, J. 2000. “Injury Mechanism of Pedestrians During a Front-End Collision with a Late Model Car”. JSAE Spring 2000.

[7] Kerrigan, J. R., Crandall, J. R. and B. Deng. 2007. "Pedestrian kinematic response to mid-sized vehicle impact." International Journal of Vehicle Safety 2(3): 221-240.
[8] Kerrigan, J., Murphy, D. B., Drinkwater, D. C., Kam, C. Y., Bose D., and Crandall, J. R. 2005. "Kinematic Corridors for PMHS Tested in Full-Scale Pedestrian Impact Tests". Enhanced Vehicle Safety (ESV), Washington D.C., US.
[9] Subit, D., Kerrigan, J., Crandall, J. R., Fukuyama, K., Yamazaki, K., Kamiji, K., and Yasuki, T. 2008. "Pedestrian-vehicle interaction: kinematics and injury analysis of four full scale tests". In Proceedings of the International Research Council on the Biomechanics of Injury conference (Vol. 36, pp. 275-294). International Research Council on Biomechanics of Injury.
[10] Simms, C., and Wood, D. 2009. "Pedestrian and cyclist impact: a biomechanical perspective" (Vol. 166). Springer Science & Business Media.
[11] Maki, T., Kajzer, J., Mizuno, K., and Sekine, Y. 2003. "Comparative analysis of vehicle-bicyclist and vehicle-pedestrian accidents in Japan". Accident Analysis and Prevention 35(6): 927-940.
[12] Soni, A., Robert, T., Rongieras, F., and Beillas, P. 2013. "Observations on pedestrian pre-crash reactions during simulated accidents". Stapp car crash journal, 57, 157-183.
[13] Peng, Y., Deck, C., Yang, J., and Willinger, R. 2012. "Effects of pedestrian gait, vehicle-front geometry and impact velocity on kinematics of adult and child pedestrian head." Int. J. Crashworthiness 1 (2012), pp. 1-9
[14] Untaroiu, C. D., Meissner, M. U., Crandall, J. R., Takahashi, Y., Okamoto, M., and Ito, O. 2009. "Crash reconstruction of pedestrian accidents using optimization techniques". International Journal of Impact Engineering, 36(2), 210-219.
[15] Tamura, A., Nakahira, Y., Iwamoto, M., Watanabe, I., Miki, K., Hayashi, S., and Yasuki, T. 2006. "The Influence of the Traction Force Due to Inertia of the Brain Mass on Traumatic Brain Injury during SUV-to-Pedestrian Impact." International Research Council on the Biomechanics of Impacts. IRCOBI.
[16] Yasuki, T., and Yamamae, Y. 2010. "Validation of Kinematics and Lower Extremity Injuries Estimated by Total Human Model for Safety in SUV to Pedestrian Impact Test". Journal of Biomechanical Science and Engineering 5(4): 340-356.
[17] Han, Y., Yang, J., Nishimoto, K., Mizuno, K., Matsui, Y., Nakane, D., and Hitosugi, M. 2012. "Finite element analysis of kinematic behaviour and injuries to pedestrians in vehicle collisions." International Journal of Crashworthiness, 17(2), 141-152.
[18] Han, Y., Yang, J., Mizuno, K., and Matsui, Y. 2012. "Effects of vehicle impact velocity, vehicle front-end shapes on pedestrian injury risk." Traffic injury prevention, 13(5), 507-518.
[19] Watanabe, R., Miyazaki, H., Kitagawa, Y., and Yasuki, T. 2011. "Research of Collision Speed Dependency of Pedestrian Head and Chest Injuries using Human FE Model (THUMS Version 4)." 22nd ESV, 11-0043.
[20] Watanabe R., Katsuhara, T., Miyazaki, H., Kitagawa, Y., and Yasuki, T. 2012 "Research of the Relationship of Pedestrian Injury to Collision Speed, Car-type, Impact Location and Pedestrian Sizes using Human FE model (THUMS Version 4)". Stapp Car Crash journal, Vol 56, pp. 269- 321.
[21] Paas, R., Davidsson, J., and Brolin, K. 2015. "Head Kinematics and Shoulder Biomechanics in Shoulder Impacts similar to Pedestrian Crashes–a THUMS study." Traffic injury prevention, 16(5):498-506. doi: 10.1080/15389588.2014.968778.
[22] Peng, Y., Deck, C., Yang, J., Otte, D., Willinger, R. 2013. "A study of adult pedestrian head impact conditions and injury risks in passenger car collisions based on real-world accident data". Traffic injury prevention, 14(6), 639-646.